Stress effects on the ESR spectra of Dy in Ag thin films

C. A. Pelá, G. E. Barberis, J. F. Suassuna, and C. Rettori
Instituto de Fiscia "Gleb Wataghin", Universidade Estadual de Campinas, 13100-Campinas-SP-Brasil
(Received 18 June 1979)

ESR experiments on dilute Ag:Dy thin films at liquid-helium temperatures allow the estimation of lower limits for the second-order orbit-lattice coupling parameters. The anisotropy observed on the g value of the Γ_7 ground state of Dy is interpreted in terms of admixtures of excited crystal-field levels with the ground state, via a planar strain of the film, induced by the difference in the thermal-expansion coefficients between the film and the substrate. The results indicate that the tetragonal orbit-lattice parameter agrees in sign with that predicted by the point-charge model, but the trigonal one does not, similar to Ag:Er thin films.

I. INTRODUCTION

The orbit-lattice interaction has been shown[1] to be the appropriate mechanism to explain the relaxation of a spin system to the bath in insulators. For dilute magnetic ions in metals, however, the relaxation via exchange between the localized moments and the conduction electrons (Korringa mechanism) is the dominant mechanism.[2] Consequently, it is not possible to obtain direct information about the orbit-lattice interaction in a metallic host by conventional measurements of ESR. Therefore, the only hope of observing this interaction will lie in the modulation of the crystal field in a known way, and analyzing the response of the system to this excitation. For phonons with $k \sim 0$, which are responsible for the direct process which is dominant at low temperatures,[3] it is possible to obtain the orbit-lattice coupling parameters (OLCP) from static-stress experiments.[4] For these experiments it is necessary to use single-crystalline samples, because, even for crystals of high symmetry, there are different parameters associated with different directions of the applied static stress. This makes the experiment difficult in the case of bulk metals, because the observed resonance arises from the impurities seated in the skin depth, where the effects of strain inhomogeneities could mask the effect.

Recent experiments[5–9] have shown that ESR measurements at liquid-helium temperatures on metallic single-crystalline thin films diluted with rare earths is a good way to estimate the OLCP of a rare-earth ion in a metallic host. The difference in thermal-expansion coefficients between the metallic film and the substrate will induce a planar strain on the former, and, as a result of this strain, an anisotropic ESR spectrum is obtained. This anisotropy allows the estimation of the OLCP.

We report a detailed ESR study on dilute Dy in Ag thin films grown on NaCl and quartz substrates. It is known[10] that the Ag-cubic-crystal field splits the $Dy^{3+}(4f^9)^6H_{15/2}$ multiplet into one Γ_7, three $\Gamma_8^{(i)}$, and one Γ_6 levels, Γ_7 being the ground state. Now, if an axial strain field is applied to the film, a small second-order crystal-field component appears, as well as even smaller new fourth- and sixth-order components of the crystal field; the $\Gamma_8^{(i)}$ levels of the $J=\frac{15}{2}$ multiplet split and mix considerably with the Γ_7 ground state, which becomes anisotropic, following the new axial symmetry of the crystal field. By doing careful measurements of the $Dy^{3+}\Gamma_7$ g-value anisotropy in Ag[001]- and [111]-oriented thin films, we were able to estimate lower limits for the tetragonal ($G_{3g}^{(2)}$) and trigonal ($G_{5g}^{(2)}$) second-order OLCP.

In Sec. II we give experimental details and results. Section III deals with phenomenological and microscopic theories. We use a spin-lattice Hamiltonian to analyze the data obtained from the experiments, and the microscopic orbit-lattice Hamiltonian to obtain the orbit-lattice parameters. In Sec. IV, we discuss the orbit-lattice interaction in terms of a point-charge model (PCM) and virtual bound states (vbs), and we make a critical analysis of our data and estimated parameters. A comment on the recent work of Dodds and Sanny,[8] and Oseroff and Calvo[11] is also given.

II. EXPERIMENTS AND RESULTS

Three different kinds of thin films were obtained by evaporating arc melted 1–2% Ag:Dy alloys. They were : [001]-oriented single crystals, grown on hot (001) NaCl cleaved surfaces; [111]-oriented single crystals, grown on hot (111) NaCl polished surfaces; and [111]-oriented films, with a mosaic structure (i.e., composed of many small crystals, all of them oriented parallel to the [111] direction with the other axes oriented at random), using amorphous quartz as a substrate, or either (001) or (111) NaCl surfaces, as long as their deposition temperatures were kept below 250 °C.

In order to get good epitaxiality on NaCl, the surfaces were treated with water vapor before deposition,[12] and the evaporating chamber was kept at a residual ultrahigh vacuum of 10^{-8} Torr. During evaporation the substrates were heated up to temperatures of about 390 °C. The deposition rates were very high (~800 Å/sec), and we evaporated just the appropriate amount of the alloy for the desired thickness, in order to get better impurity homogeneity in the film, since, as in the case of Er in Ag and Au thin films,[9] it was observed that a very small amount of rare-earth metal was evaporated from the alloy at the beginning of the evaporation.[13] When the evaporation was finished, the heater on the substrate was disconnected, and the film substrate was cooled down to room temperature in about 90 minutes; then the films were put in an inert argon atmosphere until the ESR experiment was run. No further thermal treatment was done, and in this way very good epitaxial single-crystalline films were obtained on NaCl substrates, as x-ray diffraction and electron-transmission-microscopy analysis have demonstrated. Several thicknesses were used (2000–5000 Å), showing no dependence of the results on the thickness, and only showing difficulty in observing the resonance when the thickness was thinner than 2000 Å. After a few days of being in contact with the room atmosphere, the films did not show resonance any more.

The ESR experiments were carried on in an *X*-band standard Varian spectrometer. The samples were immersed in liquid ^{4}He. A quartz-tail stainless-steel Dewar, which fits into a TE_{102} 100-KHz Varian microwave cavity kept at room temperature, was used. The temperatures were obtained by measuring the vapor pressure of the liquid helium.

Figure 1 shows a typical spectrum at 1.5 K of Ag:Dy for a film 2100-Å thick evaporated on a (111) NaCl hot surface.

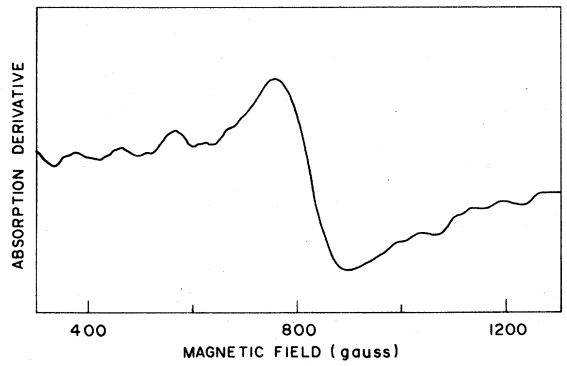

FIG. 1. ESR spectrum at 1.5 K of Dy diluted in a 2100-Å thick (111) Ag film evaporated on a NaCl (111) surface at 300 °C. The field orientation is at $\theta = 55.7°$ from the normal to the plane of the film.

Figure 2 gives the observed *g*-value anisotropies for films of Ag:Dy evaporated on (001), (111) NaCl, and quartz substrates, when the magnetic field is rotated in a plane perpendicular to the plane of the film. The solid line is a least-squares fit of

$$g(\theta) = g_0 + \tfrac{1}{2}\Delta g(3\cos^2\theta - 1) \quad (1)$$

to the experimental data. Here g_0 and Δg are the fitting parameters, and θ the angle between the magnetic field and the direction perpendicular to plane of the film. Within experimental accuracy, the linewidth, for all the analyzed films, did not show any anisotropy.

Table I gives all the fitting parameters for the analyzed films. The error bars given on these parameters were obtained from a weighted statistical average of the experimental accuracy. The deposition temperatures, and expected deformations between 1.5 K and the deposition temperatures calculated from Eq. (2) and Ref. 14 (see below), are also given.

From Table I we conclude that there are sliding effects of the film at the interface, because the anisotropies observed on the *g* value for (111) films, do not scale with the expected deformations, either for NaCl or quartz substrates. The expected deformation for hot substrates is about two times bigger than that of the cold substrate. We neglect nonlinear effects because the same behavior is observed in compression (NaCl substrate) and expansion (quartz sub-

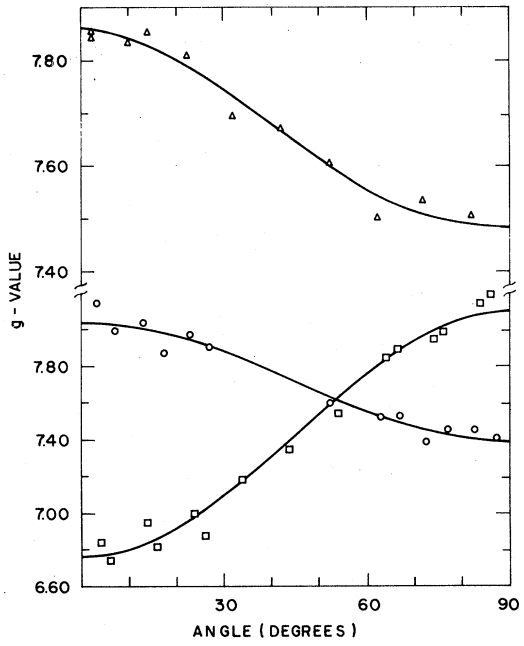

FIG. 2. Angular dependence of the *g* value of Dy in Ag thin films at 1.5 K. The triangles are the experimental values for the 5000-Å (001) film; the circles correspond to the 2100-Å (111) film; and the squares to the 2100-Å (111) film with mosaic structure on quartz substrate.

TABLE I. Experimental ESR data of Ag:Dy thin films.

Substrate	T_d[a] (K)	ϵ'_{xx}[a] (%)	g_0	Δg	Linewidth (gauss)	Thickness (Å)	Structure (x ray)
Quartz	578	0.98	7.61±0.04	−0.87±0.03	350 ± 35	2100	(111)[b]
Quartz	300	0.45	7.65±0.05	−0.88±0.04	450 ± 45	3500	(111)[b]
NaCl(001)	673	−1.70	7.61±0.01	0.26±0.02	170 ± 17	5000	(001)
NaCl(001)	300	−0.42	7.64±0.02	0.37±0.03	100 ± 10	3000	(111)[b]
NaCl(111)	578	−1.36	7.62±0.03	0.42±0.03	160 ± 16	2100	(111)

[a]Deposition temperatures and deformations are estimated within 20%.
[b]Films with mosaic structure.

strate) experiments. Therefore the deformations given in Table I are only upper limits for the films deformations.

A few films were separated from the substrate and measured again. The experiment showed an isotropic spectrum with a g value and thermal broadening of 7.63 ±0.08 and 8 ±2 G/K, respectively. These values agree with those measured in bulk,[10] and confirm that our experiments deal with properties of dilute Dy in Ag. In a few cases the thermal broadening of the linewidth for strained films was also measured. We found values close to those given above.

III. ANALYSIS AND THEORY

A. Strain induced on the films

We are going to interpret our experimental results in terms of a strain induced on the film by the difference in thermal-expansion coefficients between substrate and film. We shall use two sets of orthogonal axes to describe the strain (ϵ'_{ij} and ϵ_{ij}) and stress (σ'_{ij} and σ_{ij}) tensors. The x', y', and z' set, with z' perpendicular to the interface of the film substrate, will be the interface frame; and the other x, y, and z set, with axes parallel to the cubic crystal axes of the film, will be the crystal frame.

In order to calculate the maximum expected strains induced on the films, we are going to use the following assumptions: (i) The film is firmly attached to the substrate; (ii) the stress and the thermal expansion of the film and the substrate are isotropic at the interface ($\sigma'_{xy}=0;\epsilon'_{xy}=0$), and the thermal-expansion coefficients are given by those of the free materials; (iii) the stress on the film in the direction perpendicular to the interface is zero ($\sigma'_{zz}=0$); i.e., the film is free along this direction; and (iv) the shear strains perpendicular to the interface are zero ($\epsilon'_{xz}=\epsilon'_{yz}=0$); i.e., there is no bending effect in the plane of the film.

According to (i) and (ii) the maximum values of the strain tensor in the interface frame are given by

$$\epsilon'_{xx}=\epsilon'_{yy}=\int_{T_m}^{T_d}(\alpha_{\text{film}}-\alpha_{\text{subst}})\,dT\ , \tag{2}$$

where α_{subst} and α_{film} are the thermal-expansion coefficients of the substrate and film, respectively, which are obtained from Ref. 14, and T_d and T_m the deposition and measurement temperatures, respectively.

In order to obtain the stress and strain tensors in the crystal frame, we shall distinguish between the three following situations according to the structures obtained in our films, i.e., [001]-[111]-oriented single-crystalline films and [111]-oriented film with a mosaic structure.

1. *[001] epitaxially grown single-crystal film*

The assumption (ii) implies that any rotation around the z' axis leaves the strain and stress tensors invariant; therefore we can write

$$\epsilon_{xx}=\epsilon'_{xx} \tag{3a}$$

and

$$\epsilon_{yy}=\epsilon'_{yy}\ , \tag{3b}$$

and from assumption (iii)

$$\epsilon_{zz}=\epsilon'_{zz}=\frac{S_{12}}{S_{11}+S_{12}}(\epsilon'_{xx}+\epsilon'_{yy})=\alpha\epsilon'_{xx}\ , \tag{3c}$$

where the S_{ij} are the elastics compliances for the film, which are obtained from Ref. 14. The assumption (iv) will lead to

$$\epsilon_{ij}=0 \quad \text{for } i\neq j\ . \tag{3d}$$

2. *[111] epitaxially grown single-crystal film*

In this case we can obtain the stress and strain tensors in the crystal frame from those in the interface frame by doing three successive Euler rotations of these tensors. The first is a rotation of angle ψ about

the z' axis, which leaves the x' axis on a crystal (110) plane. As can be seen, this rotation, together with assumption (ii), leaves the strain and stress tensors invariant. The following two rotations are $\theta_0 = -55.735°$ about the crystal [110] direction and $\phi_0 = -45°$ about the crystal [001] direction.

Applying the above rotations to the strain tensor in the interface frame, and using assumptions (ii)–(iv), we can write its components in the crystal frame as follows:

$$\epsilon_{xx} = \epsilon_{yy} = \epsilon_{zz} = \frac{1}{3}(\epsilon'_{xx} + \epsilon'_{yy} + \epsilon'_{zz}) \tag{4a}$$

and

$$\epsilon_{xy} = \epsilon_{yz} = \epsilon_{xz} = \frac{1}{3}(\epsilon'_{zz} - \epsilon'_{xx}) \ . \tag{4b}$$

Now, using the elastic compliances and the inverse transformation,

$$\epsilon'_{zz} = \frac{S_{11} + 2S_{12} - S_{44}}{2S_{11} + 4S_{12} + S_{44}}(\epsilon'_{xx} + \epsilon'_{yy}) = \beta\epsilon'_{xx} \ , \tag{4c}$$

$$\epsilon_{xy} = \epsilon_{yz} = \epsilon_{xz} = \frac{1}{3}(\epsilon'_{zz} - \epsilon'_{xx}) = \frac{1}{3}(\beta - 1)\epsilon'_{xx} \ . \tag{4d}$$

3. *[111]-oriented films with mosaic structure*

Since the assumption of isotropy on the strain and stress at the interface leaves invariant the tensors under any rotation around a direction perpendicular to the film, this case can be analyzed much in the same way as was done for case 2.

In cubic symmetry it is useful to define the normal strains $\epsilon_{i,\alpha}$, which are a linear combination of the strain-tensor components transforming like the α component of a vector basis of the i-irreducible representation of the cubic point group O_h. These normal strains are

$$\begin{aligned}
\epsilon_{1g} &= \epsilon_{xx} + \epsilon_{yy} + \epsilon_{zz} \ , \\
\epsilon_{3g\theta} &= \frac{1}{2}(2\epsilon_{zz} - \epsilon_{xx} - \epsilon_{yy}) \ , \\
\epsilon_{3gn} &= \frac{\sqrt{3}}{2}(\epsilon_{xx} - \epsilon_{yy}) \ , \\
\epsilon_{5g\lambda} &= \sqrt{3}\epsilon_{yz} \ , \\
\epsilon_{5g\kappa} &= \sqrt{3}\epsilon_{xz} \ , \\
\epsilon_{5g\mu} &= \sqrt{3}\epsilon_{xy} \ ,
\end{aligned} \tag{5}$$

which can be easily calculated from Eqs. (2)–(4), together with the tabulated data for α_{subst} and α_{Ag}.[14]

B. Phenomenological theory

Ag:Dy shows only one resonance. Therefore it can be represented by the following spin Hamiltonian for an effective spin $S = \frac{1}{2}$, which includes all the symmetry properties:

$$\hat{\mathcal{H}}_s = g_{\text{eff}}\mu_B \vec{H}\cdot\vec{S} + \hat{\mathcal{H}}_{\text{SL}} \ , \tag{6}$$

where g_{eff} is the isotropic g factor expected for a doublet in cubic symmetry, μ_B is the Bohr magneton, H is the external magnetic field, and $\mathcal{H}_{\text{SL}}$ is the spin-lattice Hamiltonian which takes into account the effect of strain which distorts the cubic lattice. The spin-lattice Hamiltonian can be written[15]

$$\hat{\mathcal{H}}_{\text{SL}} = \mu_B \sum_{i,\alpha} g_i \epsilon_{i,\alpha} O_{i,\alpha}(S,H) \ , \tag{7}$$

where the $O_{i,\alpha}$ are functions of the effective spin and applied magnetic field, transforming in the same way as the normal strains $\epsilon_{i,\alpha}$, and the g_i are the phenomenological spin-lattice parameters.

For [001] thin films (case 1), using Eqs. (3), (5), and (6), we obtain the following angular variation for the g value:

$$g(\theta) = g_{\text{eff}} + g_{1g}\epsilon_{1g} + \frac{1}{2}g_{3g}\epsilon_{3g\theta}(3\cos^2\theta - 1) \ , \tag{8}$$

where θ is the angle between the magnetic field direction and the normal to the films.

Similarly for [111] thin films (cases 2 and 3), the angular dependence of the g value is given by

$$g(\theta) = g_{\text{eff}} + g_{1g}\epsilon_{1g} + \frac{1}{2}g_{5g}\epsilon_{5g}(3\cos^2\theta - 1) \ , \tag{9}$$

with

$$\epsilon_{5g} = \epsilon_{5g\kappa} = \epsilon_{5g\lambda} = \epsilon_{5g\mu} \ ,$$

for both single crystals and mosaic structure films.

Equations (8) and (9) give the same angular dependence as Eq. (1); therefore, we can now identify the parameters. We found, within our experimental accuracy, g_{1g} to be negligible, since, for all our measurements, the parameter g_0 in Eq. (1) was found to be very close to the g value of Dy in bulk alloys (see Table I). Since we have evidence that the films partially slide off from the substrate at the interface (see Sec. II), we can estimate just a lower limit for the g_{3g} and g_{5g} parameters in Eqs. (8) and (9), because Eq. (2) will give only an upper limit for the normal strains. Using the values of Δg given in Table I for [001] films and [111]-oriented films with the lowest deposition temperatures, we have estimated

$$g_{3g} \geq 6.09; \quad g_{5g} \geq 146.7 \ . \tag{10}$$

C. Microscopic theory

The Hamiltonian which describes the energy of the ground multiplet for a rare-earth paramagnetic ion in cubic symmetry is given by $\bar{\mathcal{H}} = \mathcal{H}_c + \mathcal{H}_z$, where $\mathcal{H}_c$ and

$\mathcal{H}_z$ are the cubic-crystal field and Zeeman interactions, respectively. When a strain distorts the lattice, the orbit-lattice interaction $\bar{\mathcal{H}}_{\rm OL}$ should be added to the Hamiltonian. It can be written[15]

$$\bar{\mathcal{H}}_{\rm OL}=\sum_{n,i,\alpha,\xi} G_i^{(n,\xi)} O_{i,\alpha}^{(n,\xi)} \epsilon_{i,\alpha} \ , \tag{11}$$

where the $O_{i,\alpha}^{(n,\xi)}$ are linear combinations of n-order the Stevens operators following the same transformation rules as the $\epsilon_{i,\alpha}$, and the $G_i^{(n,\xi)}$ are the orbit-lattice coupling parameters.

As previously reported,[10] dilute Dy^{3+} in Ag presents a $4f^9$ configuration with a $^6H_{15/2}$ as a lower multiplet. The cubic-crystal field splits this multiplet into one Γ_7, one Γ_6, and three $\Gamma_8^{(i)}$ levels, with Γ_7 the ground state. In this case, only a second-order process involving both $\bar{\mathcal{H}}_z$ and $\bar{\mathcal{H}}_{\rm OL}$ can modify the doublet composition, admixing the Γ_7 with the excited levels of the $J=\frac{15}{2}$ multiplet, and inducing an anisotropy of the g value. The hydrostatic term in Eq. (10) is isotropic; therefore it can only admix different Γ_7 levels; this means that in our case the admixtures should be with different J multiplets. So, we have neglected this term, based in our experimental results, which show that the g_0 value [Eq. (1)] agrees with the g value of Dy in bulk alloys.

Calculating these second-order energies with the wave functions $|\Gamma_{7a}\rangle$ and $|\Gamma_{7b}\rangle$ that diagonalize the Zeeman effect on the doublet, and considering always the z' axis perpendicular to the interface, and using Eq. (11), the Zeeman Hamiltonian for the doublet and the strain tensor in the crystal frame we have

$$g(\theta)=g_{\rm eff}+g_{\rm eff}\left(\sum_{n,i,\alpha}\frac{2G_{3g}^{(n)}\epsilon_{3g\theta}}{\langle\Gamma_{7\alpha}|J_z|\Gamma_{7\alpha}\rangle}\frac{\langle\Gamma_{7\alpha}|J_z|\Gamma_{8\mu}^{(i)}\rangle\langle\Gamma_{8\mu}^{(i)}|O_{3g\theta}^{(i)}|\Gamma_{7\alpha}\rangle}{E_7-E_8^{(i)}}\right)\frac{1}{2}(3\cos^2\theta-1)=g_{\rm eff}+\frac{1}{2}g_{3g}\epsilon_{3g\theta}(3\cos^2\theta-1) \tag{12}$$

for the [001] film, and

$$g(\theta)=g_{\rm eff}+\sqrt{3}ig_{\rm eff}\sum_{n,i,\alpha,\xi}\left(\frac{G_{5g}^{(n,\xi)}\epsilon_{5g}}{\langle\Gamma_{7\alpha}|J_z|\Gamma_{7\alpha}\rangle}\frac{\langle\Gamma_{7\beta}|J_+|\Gamma_{8\lambda}^{(i)}\rangle\langle\Gamma_{8\lambda}^{(i)}|O_{5g\mu}^{(n,\xi)}|\Gamma_{7\beta}\rangle}{E_7-E_8^{(i)}}\right)\frac{1}{2}(3\cos^2\theta-1)$$

$$=g_{\rm eff}+\frac{1}{2}g_{5g}\epsilon_{5g}(3\cos^2\theta-1) \ , \tag{13}$$

where

$$O_{3g\theta}^{(2)}=\tfrac{1}{2}[3J_z^2-J(J+1)]$$

and

$$O_{5g\mu}^{(2)}=\frac{\sqrt{3}}{4i}(J_+^2-J_-^2) \ ,$$

for the [111]-oriented crystal, where $|\Gamma_{7\alpha}\rangle$ and $|\Gamma_{7\beta}\rangle$ are the wave functions for the ground state for $\vec{H}$ parallel to the [001] axis.

The right-hand sides of Eqs. (12) and (13) are linear combinations of three and four OLCP, respectively. Therefore it is impossible to estimate each of them from our experimental data. Following Arbilly *et al.*,[5] we shall assume the second-order parameter, in both Eqs. (12) and (13), to be much bigger than the fourth- and sixth-order parameters. Then if the hydrostatic term does not induce a significant change in the cubic crystal field, we can use the crystal-field parameters and splittings given by Oseroff *et al.*[16] together with the wave functions for a perfect Russel-Saunders coupling for $x=0.53$ given by Lea, Leask, and Wolf.[17] Then Eqs. (12) and (13) give

$$g_{3g}/g_{\rm eff}=-(0.9155)G_{3g}^{(2)}$$

and

$$g_{5g}/g_{\rm eff}=5.1650G_{5g}^{(2)} \ , \tag{14}$$

where we have included the contributions of the three excited $\Gamma_8^{(i)}$ states at 11.5, 50, and 180 K from the Γ_7 ground state, respectively.

Following previous calculations for insulators, we have used the PCM developed by Sroubek *et al.*[4] to estimate the upper limit (crystal field only) for the $G_i^{(\eta,\xi)}$. For cubic fcc sites we obtain

$$G_{3g}^{(2)}=e^2e_{\rm eff}\frac{\langle r^2\rangle}{R^3}\alpha_J$$

and

$$G_{5g}^{(2)}=2e^2e_{\rm eff}\frac{\langle r^2\rangle}{R^3}\alpha_J \ , \tag{15}$$

where $e_{\rm eff}$ is the effective charge for Ag ions given in electronic charge units, and will be taken equal to 1; $\langle r^2\rangle$ is the mean-square radius for the $4f$ electrons in the Dy^{3+} ion obtained from a Hartree-Fock calculation,[18] e the electronic charge, and R the distance to the nearest neighbors.

Table II gives the lower limits of the OLCP for Ag, $G_{3g}^{(2)}$ and $G_{5g}^{(2)}$, estimated from Eqs. (10). It is interesting to note that these values are of the order of magnitude of those found in Ag:Er thin films[5,7] and that of the second-order static-crystalline-field parameter found in hexagonal metals.[19] The values of these parameters calculated from PCM are also shown.

TABLE II. Second-order orbit-lattice coupling parameters of Ag:Dy.

	Ag:Dy	PCM
$G_{3g}^{(2)}/\alpha_J$(K)	≥ 137	1041
$G_{5g}^{(2)}/\alpha_J$(K)	≤ -584	2082

IV. DISCUSSION

From Table II it is interesting to note that Dy^{3+}, (similarly to Er^{3+})[7] diluted in Ag thin films, gives a value of $G_{3g}^{(2)}$ which agree in sign with that expected from PCM, while that of $G_{5g}^{(2)}$ does not. These results are in agreement with those recently found in magnetostriction experiments by Campbell *et al.*[20] As in the case[7] of Er^{3+}, it can be suggested that, if higher order OLCP are not important, the effect of virtual bound states might be responsible for this change in sign, similar to what happens with the fourth-order static cubic-crystal field of Er^{3+} in Ag and Au[21]. However, for the case of Dy^{3+}, further experimental evidence for the change in sign is added: uniaxial stress experiments on the Γ_7 ground state of Dy^{3+} in CaF_2[15] show the same effect, where no conduction-electron effects are expected. Calvo *et al.*[15] attributed this to shielding and covalency effects. No further calculations have been done on this problem. Therefore, we believe that theoretical calculations, including shielding and covalency effects, Coulomb repulsion, and exchange interaction between the $4f$ electrons and the $5d$ and/or $5p$ vbs, taking into consideration the population, width, and the crystal-field splitting of these vbs, are needed for a better understanding of our experimental results.

It is interesting to observe that no angular variation of the linewidth has been observed for any of our Ag:Dy thin films. This means that the strains are homogeneous across the films; so we are not dealing with mean values of the deformations,[6] but in any case we can only estimate a lower limit of the OLCP, since we have evidence that the films might partially slide off of the substrate.

Recently Dodds and Sanny[8] have reported an experimental value for $G_{3g}^{(2)}$ in Ag:Dy which agrees in sign and order of magnitude with our $G_{5g}^{(2)}$ value. According to our experience, and to the way that they have grown their films, we believe that the structure of their films would have been [111]-oriented films with a mosaic structure. Consequently they could have attributed the wrong OLCP to their experiment. In any case it would be necessary to do x-ray and/or microscopy analysis on their films in order to clarify this problem.

Since the PCM gives an upper limit for the OLCP, the values recently reported by Oseroff *et al.*[11] for the width of the normal-strain distribution in their Ag:Dy single crystals can be considered as lower limits of those widths, although their values should be corrected for fcc symmetry. Now that we are able to estimate lower limits for the OLCP, we can give the following upper limits $\sigma_3 \leq 2.82 \times 10^{-2}$ and $\sigma_5 \leq 2.77 \times 10^{-3}$ for the widths of the normal-strain distributions in Ag:Dy single crystals.

Finally we conclude that the direct spin-lattice relaxation times in metallic hosts must be of the same order of magnitude as those in insulators, because the OLCP measured in metals and equivalent insulating lattices are of the same order of magnitude.[3]

ACKNOWLEDGMENTS

This research was partially supported by FAPESP and CNPq.

[1]See, for example P. L. Scott and C. D. Jeffries, Phys. Rev. 127, 32 (1962), and references therein.
[2]C. Rettori, D. Davidov, R. Orbach, and E. P. Chock, Phys. Rev. B 7, 1 (1973).
[3]R. Orbach and H. J. Stapleton, in *Electron Paramagnetic Resonance*, edited by S. Geschwind (Plenum, New York, 1972).
[4]Z. Sroubek, M. Tachiki, P. H. Zimmerman, and R. Orbach, Phys. Rev. 165, 435 (1968).
[5]D. Arbilly, G. Deutscher, E. Grunbaum, R. Orbach, and J. T. Suss, Phys. Rev. B 12, 5068 (1975).
[6]J. F. Suassuna, G. E. Barberis, C. Rettori, and C. A. Pelá, Solid State Commun. 22, 347 (1977).
[7]G. E. Barberis, J. F. Suassuna, C. Rettori, and C. A. Pelá, Solid State Commun. 23, 603 (1977).
[8]S. A. Dodds and J. Sanny, Phys. Rev. B 18, 39 (1978).
[9]C. A. Pelá, G. E. Barberis, J. F. Suassuna, and C. Rettori, Phys. Rev. B (to be published).
[10]D. Davidov, C. Rettori, A. Dixon, K. Baberschke, E. P. Chock, and R. Orbach, Phys. Rev. B 8, 3563 (1973).
[11]S. Oseroff and R. Calvo, Phys. Rev. B 18, 3041 (1978).
[12]D. Walton, T. N. Rhodin, and R. W. Rollins, Chem. Phys. 38, 2698 (1963).
[13]C. A. Pelá, Ph. D. thesis [Instituto de Física, UNICAMP, Campinas (S. P.) Brazil, 1979] (unpublished).
[14]*American Handbook of Physics*, 2nd ed. (McGraw Hill, New York, 1963).
[15]R. Calvo, S. Oseroff, C. Fainstein, M. Passeggi, and M. Tovar, Phys. Rev. B 9, 4888 (1974).
[16]S. Oseroff, M. Passesggi, D. Wohlleben, and S. Shultz, Phys. Rev. B 15, 1283 (1977).
[17]K. R. Lea, M. J. M. Leask, and W. P. Wolf, J. Phys. Chem. Solids, 23, 1381 (1962).
[18]A. J. Freeman and R. E. Watson, Phys. Rev. 127, 2058 (1962).
[19]P. Touburg and J. Høg, Phys. Rev. Lett. 33, 775 (1974).
[20]I. A. Campbell, G. Creuzet, and J. Sanchez, Phys. Rev. Lett. 43, 234 (1979).
[21]G. Williams and L. L. Hirst, Phys. Rev. 185, 407 (1979).